electronic reprint

Journal of
Synchrotron Radiation
ISSN 0909-0495

Evidence for the formation of disulfide radicals in protein crystals upon X-ray irradiation

Martin Weik, Jacqueline Bergès, Maria L. Raves, Piet Gros, Sean McSweeney, Israel Silman, Joel L. Sussman, Chantal Houée-Levin and Raimond B. G. Ravelli

Copyright © International Union of Crystallography

Author(s) of this paper may load this reprint on their own web site provided that this cover page is retained. Republication of this article or its storage in electronic databases or the like is not permitted without prior permission in writing from the IUCr.

Evidence for the formation of disulfide radicals in protein crystals upon X-ray irradiation†

Martin Weik,[a]* Jacqueline Bergès,[b] Maria L. Raves,[c] Piet Gros,[d] Sean McSweeney,[e] Israel Silman,[f] Joel L. Sussman,[g] Chantal Houée-Levin[h] and Raimond B. G. Ravelli[i]

[a]Institut de Biologie Structurale, Laboratoire de Biophysique Moléculaire, 38027 Grenoble, France, [b]Laboratoire de Chimie Théorique, Université P. et M. Curie, 4 Place Jussieu, 75230 Paris, France, [c]Department of NMR Spectroscopy, Bijvoet Center for Biomolecular Research, Utrecht University, 3584 CH Utrecht, The Netherlands, [d]Department of Crystal and Structural Chemistry, Bijvoet Center for Biomolecular Research, Utrecht University, 3584 CH Utrecht, The Netherlands, [e]ESRF, BP 220, 38043 Grenoble, France, [f]Department of Neurobiology, Weizmann Institute of Science, Rehovot 76100, Israel, [g]Department of Structural Biology, Weizmann Institute of Science, Rehovot 76100, Israel, [h]Laboratoire de Chimie Physique, Université de Paris-Sud, 91405 Orsay, France, and [i]EMBL Outstation, 38042 Grenoble, France. E-mail: weik@ibs.fr

Irradiation of proteins with intense X-ray radiation produced by third-generation synchrotron sources generates specific structural and chemical alterations, including breakage of disulfide bonds and decarboxylation. In this paper, disulfide bond lengths in irradiated crystals of the enzyme *Torpedo californica* acetylcholinesterase are examined based on quantum simulations and on experimental data published previously. The experimental data suggest that one disulfide bond elongates by ~0.7 Å upon X-ray irradiation as seen in a series of nine data sets collected on a single crystal. Simulation of the same bond suggests elongation by a similar value if a disulfide-radical anion is formed by trapping an electron. The absorption spectrum of a crystal irradiated under similar conditions shows a peak at ~400 nm, which in aqueous solution has been attributed to disulfide radicals. The results suggest that the formation of disulfide radicals in protein crystals owing to X-ray irradiation can be observed experimentally, both by structural means and by absorption spectroscopy.

Keywords: radiation damage; disulfide radicals; protein crystallography; microspectrophotometry; quantum chemical calculations.

1. Introduction

The effects of radiation damage, even though greatly mitigated by the advent of cryo-techniques, remain an inherent problem in X-ray crystallography. Besides non-specific effects, such as a reduction in diffraction power, radiation damage to protein crystals can be highly specific. Data collected at cryo-temperatures at undulator beamlines of a third-generation synchrotron source have provided evidence for disulfide bond cleavage, decarboxylation of acidic residues (Burmeister, 2000; Ravelli & McSweeney, 2000; Weik *et al.*, 2000), alterations of cysteine, methionine (Burmeister, 2000; Weik, Ravelli *et al.*, 2001) and tyrosine (Burmeister, 2000) residues, and changes at the active sites of enzymes (Burmeister, 2000; Weik, Ravelli *et al.*, 2001). Cleaved disulfide bonds were also observed in data collected at room temperature at a second-generation synchrotron source (Helliwell, 1988). Although most of the studies focused on protein crystals, damage to lipid membranes has also been reported (Cherezov *et al.*, 2000). In the light of the renewed importance of radiation damage, the relation between crystal size and the amount of useful data that can be collected has been addressed (Teng & Moffat, 2000; Glaeser *et al.*, 2000), and data-collection strategies have been revisited (Rice *et al.*, 2000).

If we want to exploit fully the brightest synchrotron sources, efforts must be made to improve our understanding of radiation damage to crystalline biological macromolecules and to design ways to minimize it. A wealth of information is available from the fields of radiation chemistry and biology that has not been taken advantage of by X-ray crystallographers. Disulfide bonds have been shown to be the most radiation-sensitive moieties in several proteins that contain them (Burmeister, 2000; Ravelli & McSweeney, 2000; Schroder-Leiros *et al.*, 2001; Weik *et al.*, 2000). Upon capture of an electron, they form disulfide radical anions, $RSSR^{\bullet-}$, which can undergo spontaneous and reversible bond rupture (Armstrong, 1990; Favaudon *et al.*, 1990; von Sonntag, 1990). Protonation of this radical leads to the formation of the disulfide radical $RSSRH^{\bullet}$, with a concomitant shift of the equilibrium towards the broken state (Armstrong, 1990). Upon rupture, a thiol, RSH, and a thiyl radical, $RS^{\bullet}$, are formed. Flexibility of the bond partners is thought to influence the equilibrium between the open and the closed forms (Favaudon *et al.*, 1990; von Sonntag, 1990), suggesting that the immediate structural environment may influence the susceptibility to radiation of a disulfide bond (Favaudon *et al.*, 1990; Ravelli & McSweeney, 2000). Solvent accessibility also seems to be one of the parameters that affect the radiation sensitivity of a disulfide bond. The most solvent-accessible disulfide bond in hen egg-white lysozyme, that between Cys6 and Cys127, has been shown by X-ray crystallography (Ravelli & McSweeney, 2000; Weik *et al.*, 2000) and γ-radiolysis (Bergès *et al.*, 1997) to be the most radiation sensitive. Another example in which high solvent accessibility pairs with increased radiation sensitivity is the Cys254—Cys265 disulfide bond in crystals of the enzyme *Torpedo californica* acetylcholinesterase (*Tc*AChE; Ravelli & McSweeney, 2000; Weik *et al.*, 2000).

Using a quantum-chemical approach, Bergès and co-workers (Bergès *et al.*, 2000) calculated the geometry of model disulfide bonds and their radicals. They determined the S—S distances to be 2.1, 2.8 and 3.5 Å in H_2S_2, $H_2S_2^{\bullet-}$ and $H_3S_2^{\bullet}$, respectively. Electron capture thus weakens the disulfide bond, which becomes intermediate between a covalent bond and a van der Waals interaction. On protonation, the S—S distance grows even larger, to a value that suggests pure van der Waals interaction of the two S atoms. Measurement of $S\gamma—S\gamma$ distances for disulfide bonds in irradiated crystalline proteins might, therefore, permit detection of disulfide radicals. Another way to detect disulfide radicals is by taking advantage of their characteristic absorption spectrum (Favaudon *et al.*, 1990). Here we further analyse data from a previous study (Weik *et al.*, 2000) in which changes in disulfide bonds upon X-ray irradiation were established qualitatively. By including S atoms in the model refinement, we now provide a quantitative analysis that reveals disulfide elongation, suggesting creation of disulfide-radical anions in *Tc*AChE upon X-ray irradiation. Microspectrophotometric data and quantum-chemical calculations are presented that support this conclusion.

† Presented at the 'Second International Workshop on Radiation Damage to Crystalline Biological Samples' held at Advanced Photon Source, Chicago, USA, in December 2001.

 © 2002 International Union of Crystallography • Printed in Great Britain – all rights reserved

electronic reprint

Table 1
Energies, electron affinities, and Sγ—Sγ and C—Sγ bond lengths of the optimized cystines in their neutral and anionic forms.

Disulfide		Energy (a.u.)	Electronic affinity (eV)	Distance Sγ—Sγ (Å)	Distance C—Sγ (Å)
Cys67—Cys94	Neutral	−1289.54230	0.88	2.06	1.83
	Anion	−1289.57455		2.80	1.82
Cys254—Cys265	Neutral	−1289.53910	0.85	2.06	1.82
	Anion	−1289.57024		2.82	1.82
Cys402—Cys521	Neutral	−1289.53910	0.97	2.06	1.82
	Anion	−1289.57479		2.84	1.82

2. Materials and methods

2.1. Data collection, processing and structure refinement

Data collection and processing, dose calculation, and the starting model used for refinement are the same as described in an earlier study (Weik *et al.*, 2000). In that study, nine complete data sets, (*A*)–(*I*), were collected at 100 K from a single crystal of *Tc*AChE on the undulator beamline ID14-EH4 ($\lambda = 0.93$ Å) at the European Synchrotron Radiation Facility (ESRF) in Grenoble with a total absorbed dose of 10^7 Gy per data set. The resolution decreased from 2.1 Å in the first (*A*) to 3.0 Å in the last (*I*) data set. Whereas in our previous study all S atoms involved in disulfide bond formation were excluded from the model, and the difference density around these atoms was only interpreted qualitatively, we have now included all S atoms in order to obtain quantitative information concerning changes in disulfide geometry during the collection of sequential data sets. The S atoms were not restrained to form disulfide bonds, and their van der Waals radii were set to zero in order to avoid repulsion. Refinement utilized the *CNS* program (Brünger *et al.*, 1998). Refinement statistics differed only slightly from those presented in our previous study.

2.2. Irradiation of *Tc*AChE crystals and microspectrophotometry

A *Tc*AChE crystal of dimensions $0.15 \times 0.15 \times 0.05$ mm, grown from 34% polyethyleneglycol 200, 0.3 *M* morpholinoethanesulfonic acid, pH 5.8, was flash-cooled in the cryostream of a cooling device (600 series, Oxford Cryosystems, Oxford, UK) operating at 100 K. The crystal was continuously irradiated by X-rays of wavelength 0.93 Å for 800 s on the undulator beamline ID14-EH2 at the ESRF with concomitant rotation around the φ axis of 120°. The synchrotron was operated in uniform-fill mode and at a storage-ring intensity of ~200 mA. The X-ray beam, defined by 200×200 µm slits, was characterized by a flux of $\sim 5 \times 10^{11}$ photons s^{-1}. These values, together with a calculated absorption coefficient of 0.25 mm^{-1} and a crystal density of 1.133 g cm^{-3} (Weik, Ravelli *et al.*, 2001), resulted in a calculated total absorbed dose of 6.4×10^6 Gy. The crystal was then plunged into liquid nitrogen and mounted in the cryostream of a cooling device (600 series, Oxford Cryosystems, operating at 100 K) on an offline microspectrophotometer operating with a deuterium light source (Bourgeois *et al.*, 2002). The spectrum was recorded approximately 90 min after the termination of X-ray exposure and represents an average over ten spectra, each recorded with an integration time of 100 ms. A control spectrum of an unirradiated crystal of *Tc*AChE was recorded with identical settings.

2.3. Computational procedure

For *ab initio* calculations (Atkins, 1990), only molecules derived from cystines (in which the carboxylic group was replaced by an aldehyde group) were considered. The starting geometries for optimization of neutral disulfides and for anions were taken from the native *Tc*AChE structure (PDB code ID 1EA5) cut off at each peptide bond. All isolated disulfides were fully optimized using large basis sets (6–31+G*) at the MP2 level (Head-Gordon *et al.*, 1988) using the program *GAUSSIAN*98 (Frisch *et al.*, 1998). Our previous work demonstrated the necessity of using such large basis sets (Bergès *et al.*, 2000; Carles *et al.*, 2001). Calculations were performed on the Nec SX-5 of IDRIS (Orsay, France) and required more than 50 h for each full optimization.

3. Results

Fig. 1 shows the electron density and models for the three disulfide bonds in *Tc*AChE for the first (*A*) and the last (*I*) data sets. Disulfide bonds Cys402—Cys521 and Cys67—Cys94 are still reasonably well defined by their electron density after collection of (*I*), whereas Cys254Sγ—Cys265Sγ is clearly broken. Fig. 2 shows the Sγ—Sγ distance in the three disulfide bonds as a function of the data sets collected. The three Sγ—Sγ distances in (*A*) refine to values between 2.2 Å and 2.4 Å. The Sγ—Sγ distance in Cys402—Cys521 increases from 2.4 Å in (*A*) to a constant value of about 3.1 Å in (*G*)–(*I*). The Sγ—Sγ distance for Cys254—Cys265 can only be given for the first data set, since by the second data set Cys265Sγ is no longer defined by electron density. The Sγ—Sγ distance for Cys67—Cys94 varies between 2.2 Å and 2.5 Å, with an overall tendency to increase as a function of the data sets collected. That the observed elongations of the Sγ—Sγ bonds of Cys402—Cys521 and Cys67—Cys94 are indeed real effects, and not the result of a refinement artifact caused by loss of definition, was shown by performing structure refinements in which the disulfide bonds were specified to exist and the van der Waals radii of the S atoms were set to non-zero values. F_o–F_c maps based on this latter refinement showed negative difference density at the bond position between the two S atoms and positive difference density close to Cys521Sγ (Fig. 3) and Cys67Sγ (data not shown). This strengthens the conclusion drawn from Fig. 2 that both Cys402—Cys521 and Cys67—Cys94 elongate under our experimental conditions. Furthermore, it reveals that the largest contribution to elongation is caused by the movements of Cys521Sγ and Cys67Sγ, respectively.

The three cystines in *Tc*AChE, both in their neutral and in their anionic forms, were fully optimized in a theoretical approach based on quantum chemistry by calculating their state of minimal energy. Optimization of Cys254—Cys265 and Cys402—Cys521 in their neutral forms yields the same geometry. However, all radical geometries are different. The energies of the neutral and anionic forms are given in Table 1, together with the electronic affinities (EA). After optimization of the neutral cystines, Cys67—Cys94 has the lowest energy. Cystines Cys402—Cys521 and Cys254—Cys265 have equal energies that are 2 kcal mol^{-1} higher than that of Cys67—Cys94. The order of the anions' energies is Cys402—Cys521 < Cys67—Cys94 < Cys254—Cys265. EAs of cystines cannot be measured. However, experimental determinations of the EA in dimethyl or diethyl disulfides have shown good agreement with computed values (Carles *et al.*, 2001). The EA is highest for Cys402—Cys521 and lowest for Cys254—Cys265.

The optimized geometry of the Cys402—Cys521 cystine in its anionic form and the experimental geometry after the collection of (*I*) are very similar (Figs. 4*a* and 4*b*). However, the experimental and optimized conformations of the neutral Cys402—Cys521 are very different (Figs. 4*c* and 4*d*). Disulfide and C—Sγ bond lengths are summarized in Table 1. The calculated Sγ—Sγ bond lengths are ~2.1 Å in the neutral and ~2.8 Å in the anionic species, in agreement

electronic reprint

with previous calculations on smaller disulfides (Bergès *et al.*, 1997, 2000). The C—S bond lengths remain constant in all species, showing that electron localization occurs only on the disulfide bond.

Fig. 5 shows the absorption spectrum of a *Tc*AChE crystal after X-ray irradiation with a total absorbed dose of 6.4×10^6 Gy. A small but significant peak is visible with a maximum at 400 nm. This peak is absent in the spectrum of a non-irradiated *Tc*AChE crystal (Fig. 5).

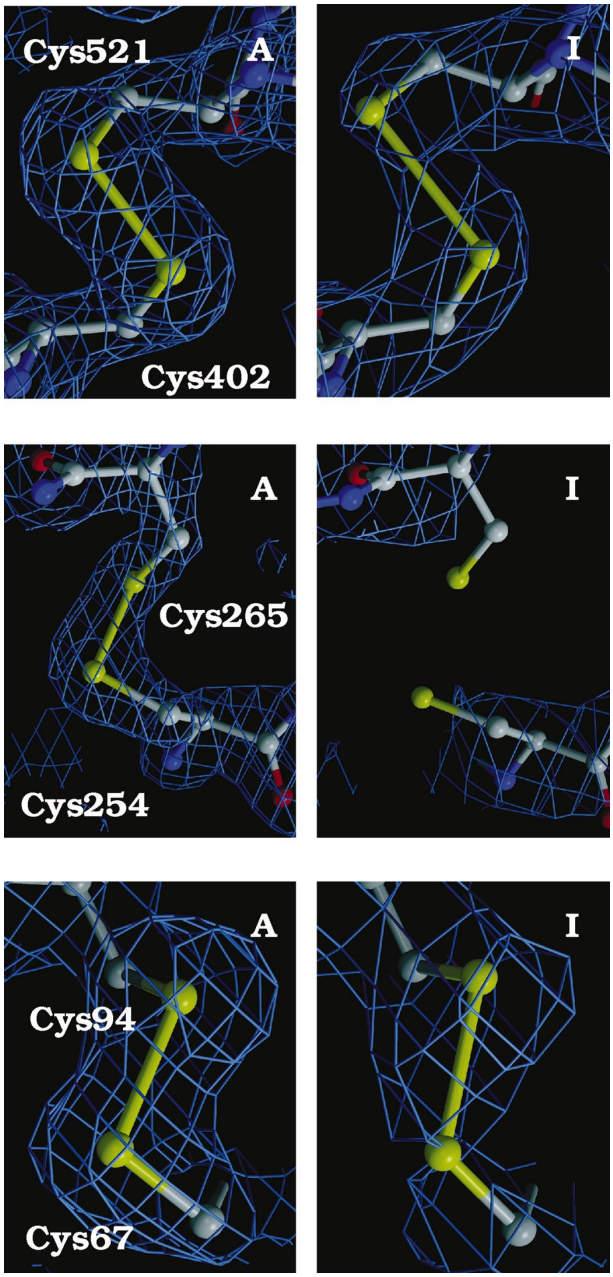

Figure 1
Electron-density maps and models for the three disulfide bonds in *Tc*AChE, *viz.* Cys402—Cys521, Cys254—Cys265 and Cys67—Cys94, for the first (*A*) and last (*I*) of a series of nine data sets collected on a single crystal at 100 K. Electron-density maps are contoured at a level of 1.5σ. During structure refinement, the S atoms were not restrained to form disulfide bonds and their van der Waals radii were set to zero in order to avoid repulsion. The programs *MOLSCRIPT* (Kraulis, 1991), *BOBSCRIPT* (Kraulis, 1991; Esnouf, 1999) and *RASTER3D* (Merritt & Bacon, 1997) were used to produce figures from electron-density maps calculated using *CNS* (Brünger *et al.*, 1998).

4. Discussion

Reexamining published data on radiation-damaged crystals of *Tc*AChE allowed us to assess the variation in Sγ—Sγ distances of disulfide bonds during data collection using a third-generation synchrotron source. The three disulfide bonds respond differently to irradiation. The distance between Cys402Sγ and Cys521Sγ elongates by 0.7 Å, whereas that between Cys67Sγ and Cys94Sγ increases by only 0.3 Å. The Cys254—Cys265 disulfide is clearly broken early in the data-collection series, without displaying any elongation in the refined model of (*A*). These data suggest an order in radiation

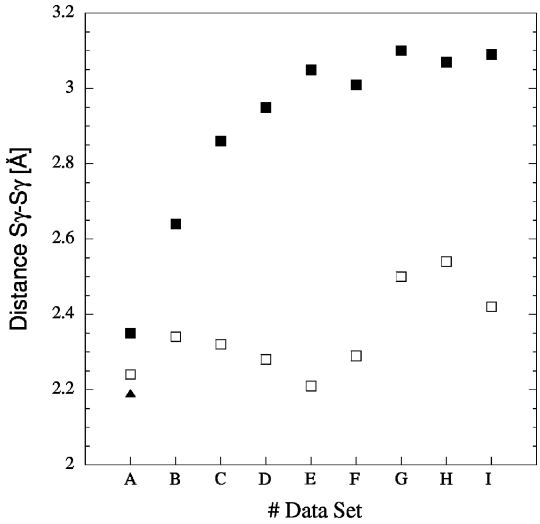

Figure 2
Sγ—Sγ distance as a function of data sets collected for Cys402—Cys521 (closed squares), Cys67—Cys94 (open squares) and Cys254—Cys265 (closed triangle).

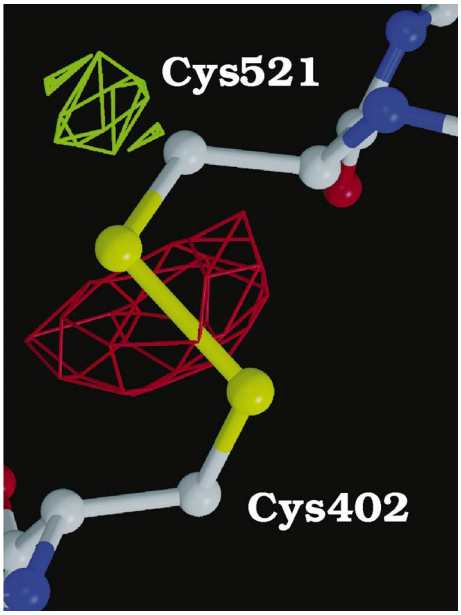

Figure 3
$F_o - F_c$ map and model of the Cys402—Cys521 disulfide bond for the fifth data set (*E*) of a series of nine data sets collected. Positive (4σ) and negative (−4σ) contours are shown in green and red, respectively. During structure refinement, the disulfide bonds were specified to exist and a van der Waals radius of 2.08 Å was used for the S atoms.

electronic reprint

sensitivity of the three disulfide bonds, with Cys67—Cys94 being the most and Cys254—Cys265 the least resistant bond, as reported earlier (Ravelli & McSweeney, 2000; Weik *et al.*, 2000).

Ab initio calculations of isolated cystines yield equilibrium geometries, corresponding energies of the optimized molecules and electron affinities that can be compared with experimental observations. The experimentally observed order in radiation sensitivity parallels the order of calculated energies in neutral cystines, which is lowest for Cys67—Cys94. Calculated Sγ—Sγ distances in the disulfide-radical anions show a similar elongation in all three disulfides (~0.7 Å with respect to those in the corresponding neutral species) yet a difference in the energies that characterize the optimized radical anions. Cys402—Cys521 forms the most stable radical anion (lowest energy) and Cys254—Cys265 the least stable. The higher EA of the former indicates that it is preferentially reduced.

The Cys67—Cys94 disulfide bond is most likely to remain predominantly in the neutral form, since it elongates only slightly upon irradiation. Even at 155 K, this bond remains radiation resistant (Weik, Ravelli *et al.*, 2001). In contrast, Cys254—Cys265 ruptures readily under our experimental conditions, and calculations suggest it to be the least stable of the three cystines in *Tc*AChE, in both its neutral and its anionic forms. In addition, increased flexibility of the two bond partners, which are located at the protein surface, and high solvent accessibility of this bond favour both radical attack and proton transfer from the solvent area and facilitate protonation of the disulfide-radical anion, thus quickly leading to destabilization and bond rupture.

The experimentally observed elongation by 0.7 Å of Cys402Sγ—Cys521Sγ is in agreement with the calculated value. It is therefore tempting to suggest that this disulfide bond forms a radical anion at 100 K. A steadily increasing elongation of the Sγ—Sγ bond during irradiation, leveling off at a value of 0.7 Å, strongly indicates that towards the end of the data-collection series the Cys402—Cys521 bond is predominantly in the anionic form. Reduced flexibility of the environment at 100 K might prevent this specific bond from breaking. Indeed, increasing the flexibility by raising the temperature to 155 K, a temperature close to the solvent glass transition in *Tc*AChE crystals (Weik, Kryger *et al.*, 2001), has been reported to result in the breaking of this bond (Weik, Ravelli *et al.*, 2001). Experimental and simulated conformations of the anion are very similar (Figs. 4*a* and 4*b*), indicating that electron localization induces little reorganization. The conformation of Cys402—Cys521 in *Tc*AChE seems, therefore, to be such that a radical anion can easily be accommodated without inducing too much strain in the polypeptide chain.

The assignment of the elongated disulfide bond to a radical anion has to be taken with caution, as multiple conformations are difficult to observe at the resolution of the present study. It is possible that a mixture of radical species of the bond is formed within the crystal and that the observed elongation thus corresponds to a mean value. Higher-resolution studies will be required to separate the elongations involved in the formation of different disulfide-radical species.

Disulfide radicals can be identified spectroscopically. Pulse radiolysis experiments have revealed that the disulfide-radical anion and its protonated form absorb with maxima at 425–440 nm and 400 nm, respectively (Favaudon *et al.*, 1990). The broad band in the absorption spectrum of irradiated *Tc*AChE crystals might, therefore, originate from disulfide radicals that are created during irradiation. The same band is visible after irradiating crystals of other disulfide-containing proteins, crystallized under various conditions (unpublished results; Murray & Garman, 2002). In contrast, absorption spectra of various protein crystals that lack disulfides, irradiated under similar conditions, lack the characteristic band at 400 nm (unpublished results). The peak maximum at 400 nm seems to indicate the presence of protonated disulfide radicals rather than disulfide-radical anions. However, the position of the absorption maximum of the disulfide-radical anion has been described as being subject to large variations (Favaudon *et al.*, 1990). Moreover, the latter study was carried out at room temperature and in aqueous solution. The effects of solvent and temperature on absorption spectra of disulfide radicals are not known. The possibility cannot be excluded that the spectrum in Fig. 5 originates from another radical species created either in the protein itself or in the crystal solvent. Methionyl (Hiller *et al.*, 1981; Bobrowski & Holcman, 1989) and tyrosinyl (Bansal & Fessenden, 1976) radicals have been described in the literature as absorbing at ~400 nm. Methionine residues can form three-electron bonds with C, N or O atoms if oxidized by $OH^{\bullet}$ radicals. The resulting radical

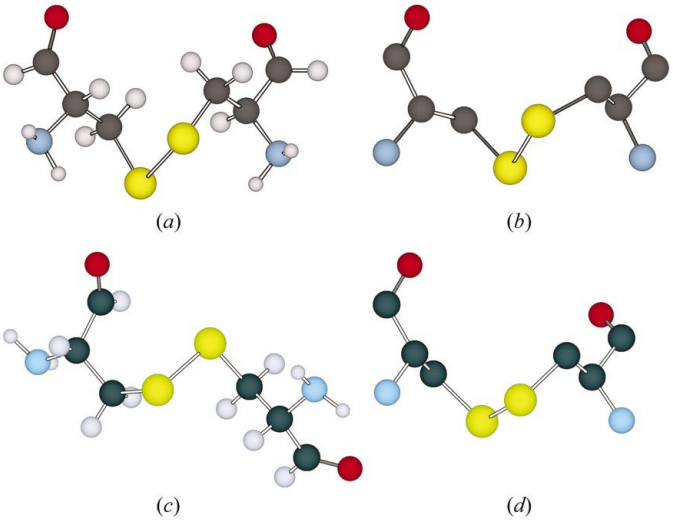

Figure 4
Simulated geometry of the Cys402—Cys521 disulfide bond in its anionic (*a*) and its neutral (*c*) state. The experimental geometry of Cys402—Cys521 for the last (*I*) of a series of nine data sets collected is represented in (*b*). (*d*) shows the experimental geometry of Cys402—Cys521 after the collection of one data set (from PDB file ID 1EA5).

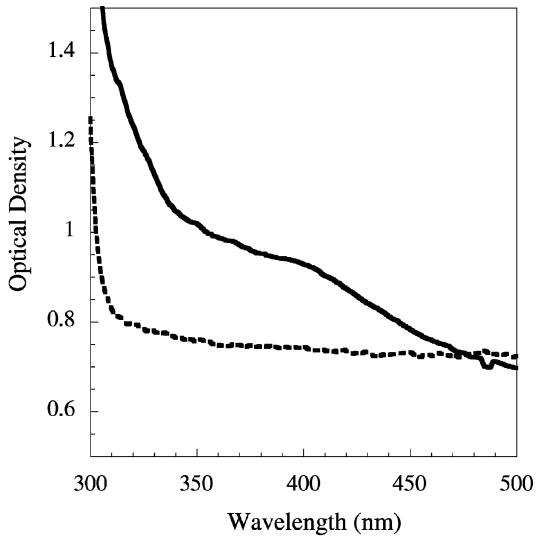

Figure 5
Absorption spectra of irradiated (solid line) and non-irradiated (dashed line) *Tc*AChE crystals.

electronic reprint

species would absorb at 390–400 nm but have not yet been observed in proteins. To date, no signs of damage due to $OH^{\bullet}$ radicals have been reported in structural radiation-damage studies at 100 K. This is probably due to the quasi-infinite viscosity of the crystal solvent at this temperature, which limits diffusion of $OH^{\bullet}$ radicals. However, methionyl-radical cations could also be created in the solid phase by hole localization. For *Tc*AChE, structural studies involving a total absorbed dose similar to that employed in the present irradiation-absorption spectroscopy experiments did not reveal any sign of damage to methionine residues at 100 K (Weik, Ravelli *et al.*, 2001). The absorption spectrum of tyrosinyl radicals displays maxima at 395 nm and 407 nm and is very narrow, thus exhibiting a clear-cut difference from the one shown in Fig. 5. Accordingly, we feel that it is indeed plausible to assign the characteristic absorption spectrum of irradiated *Tc*AChE crystals to the presence of disulfide radicals. Studies on disulfide-containing protein crystals as a function of pH (which should affect the relative amounts of $RSSR^{\bullet-}$ and $RSSRH^{\bullet}$ formed) are needed before the observed absorption spectrum can be assigned firmly to a specific disulfide-radical species.

It should be emphasized that the total absorbed dose in the irradiation-absorption spectroscopy experiment corresponds approximately to the dose required to collect one data set in the data-collection series. While damage to disulfide bonds can hardly be detected in (*A*) (Fig. 1), it is already clearly revealed in the absorption spectrum (Fig. 5). The design of strategies that aim to mitigate radiation damage may, therefore, profit from microspectrophotometry. Obviously, an online device would be crucial for real-time absorption measurements.

A technical point arising from the present study concerns the suggestion that the $S\gamma-S\gamma$ lengths of disulfide bonds should be included as a parameter in structure-refinement protocols. A value deviating from the theoretical one, *i.e.* 2.08 Å, might hint at the formation of disulfide radicals, thus yielding information concerning both the stability of the bond's environment and the solvent accessibility.

This study presents novel structural information about primary electron localization in disulfide bonds of proteins in the solid state after X-ray irradiation. The three disulfide bonds in *Tc*AChE responded differently to irradiation. The disulfide bond between Cys402 and Cys521 was elongated by ~0.7 Å as determined by protein crystallography. *Ab initio* calculations showed that this bond elongates by a similar value if an electron is trapped, suggesting that the experimentally observed elongation is due to the formation of a disulfide-radical anion. Experimentally, Cys67—Cys94 proved to be radiation resistant, and this is attributed to reduced flexibility of its environment and solvent inaccessibility. Cys254—Cys265 was readily ruptured under our experimental conditions, probably because of its high solvent accessibility and flexibility. The experimentally observed order in radiation sensitivity of the three cystines is in line with calculated energies for their neutral and anionic forms. Microspectrophotometric experiments on an irradiated *Tc*AChE crystal support the notion that disulfide radicals were formed.

We thank Dominique Bourgeois for access to the microspectrophotometer. We are grateful to Elspeth Garman for critical and constructive reading of the manuscript and fruitful discussions. James Murray is acknowledged for stimulating discussions. This work was partially funded by the Centre National d'Etudes Spatiales (contract number 793/2001/CNES/8860). We thank IDRIS for computer time (project 020168) and the ESRF (Grenoble) for access to their facilities. MW thanks the European Molecular Biology Organization for a long-term fellowship during the initial stages of this work.

References

Armstrong, D. A. (1990). *Sulfur-Centered Reactive Intermediates in Chemistry and Biology*, edited by C. Chatgilialoglu & K.-D. Asmus, pp. 121–134. New York: Plenum Press.

Atkins, P. W. (1990). *Molecular Quantum Mechanics*, 2nd ed. Oxford University Press.

Bansal, K. M. & Fessenden, R. W. (1976). *Radiat. Res.* **67**, 1–8.

Bergès, J., Fuster, F., Jacquot, J.-P., Silvi, B. & Houée-Levin, C. (2000). *Nukleonika*, **45**, 23–30.

Bergès, J., Kassab, E., Conte, D., Adjadj, E. & Houée-Levin, C. (1997). *J. Phys. Chem.* A**101**, 7809–7817.

Bobrowski, K. & Holcman, J. (1989). *J. Phys. Chem.* **93**, 6381–6387.

Bourgeois, D., Vernede, X., Adam, V., Fioravanti, E. & Ursby, T. (2002). *J. Appl. Cryst.* **35**, 319–326.

Brünger, A. T., Adams, P. D., Clore, G. M., DeLano, W. L., Gros, P., Grosse-Kunstleve, R. W., Jiang, J. S., Kuszewski, J., Nilges, M., Pannu, N. S., Read, R. J., Rice, L. M., Simonson, T. & Warren, G. L. (1998). *Acta Cryst.* D**54**, 905–921.

Burmeister, W. P. (2000). *Acta Cryst.* D**56**, 328–341.

Carles, S., Desfrançois, C., Schermann, J. P., Bergès, J. & Houée-Levin, C. (2001). *Int. J. Mass Spectrom.* **205**, 227–232.

Cherezov, V., Cheng, A., Petit, J. M., Diat, O. & Caffrey, M. (2000). *Cell Mol. Biol.* **46**, 1133–1145.

Esnouf, R. M. (1999). *Acta Cryst.* D**55**, 938–940.

Favaudon, V., Tourbez, H., Houée-Levin, C. & Lhoste, J. M. (1990). *Biochemistry*, **29**, 10978–10989.

Frisch, M. J., Trucks, G. W., Schlegel, H. B., Scuseria, G. E., Robb, M. A., Cheeseman, J. R., Zakrzewski, V. G., Montgomery, J. A., Stratmann, R. E., Burant, J. C., Dapprich, S., Millam, J. M., Daniels, A. D., Kudin, K. N., Strain, M. C., Farkas, O., Tomasi, J., Barone, V., Cossi, M., Cammi, R., Mennucci, B., Pomelli, C., Adamo, C., Clifford, S., Ochterski, J., Petersson, G. A., Ayala, P. Y., Cui, Q., Morokuma, K., Malick, D. K., Rabuck, A. D., Raghavachari, K., Foresman, J. B., Cioslowski, J., Ortiz, J. V., Baboul, A. G., Stefanov, B. B., Liu, G., Liashenko, A., Piskorz, P., Komaromi, I., Gomperts, R., Martin, R. L., Fox, D. J., Keith, T., Al-Laham, M. A., Peng, C. Y., Nanayakkara, A., Challacombe, M., Gill, P. M. W., Johnson, B., Chen, W., Wong, M. W., Andres, J. L., Gonzalez, C., Head-Gordon, M., Replogle, E. S. & Pople, J. A. (1998). *Gaussian*98. Revision A.9. Gaussian Inc., Pittsburgh PA, USA.

Glaeser, R., Facciotti, M., Walian, P., Rouhani, S., Holton, J., MacDowell, A., Celestre, R., Cambie, D. & Padmore, H. (2000). *Biophys. J.* **78**, 3178–3185.

Head-Gordon, M., Pople, J. A. & Frisch, M. J. (1988). *Chem. Phys. Lett.* **153**, 503.

Helliwell, J. R. (1988). *J. Cryst. Growth*, **90**, 259–272.

Hiller, K.-O., Masloch, B., Göbl, M. & Asmus, K.-O. (1981). *J. Am. Chem. Soc.* **103**, 2734–2743.

Kraulis, P. (1991). *J. Appl. Cryst.* **24**, 946–950.

Merritt, E. A. & Bacon, D. J. (1997). *Methods Enzymol.* **277**, 505–524.

Murray, J. & Garman, E. (2002). *J. Synchrotron Rad.* **9**, 347–354.

Ravelli, R. B. & McSweeney, S. M. (2000). *Struct. Fold. Des.* **8**, 315–328.

Rice, L. M., Earnest, T. N. & Brünger, A. T. (2000). *Acta Cryst.* D**56**, 1413–1420.

Schroder Leiros, H. K., McSweeney, S. M. & Smalas, A. O. (2001). *Acta Cryst.* D**57**, 488–497.

Sonntag, C. von (1990). *Sulfur-Centered Reactive Intermediates in Chemistry and Biology*, edited by C. Chatgilialoglu & K.-D. Asmus, pp. 359–366. New York: Plenum Press.

Teng, T. & Moffat, K. (2000). *J. Synchrotron Rad.* **7**, 313–317.

Weik, M., Kryger, G., Schreurs, A. M., Bouma, B., Silman, I., Sussman, J. L., Gros, P. & Kroon, J. (2001). *Acta Cryst.* D**57**, 566–573.

Weik, M., Ravelli, R. B., Kryger, G., McSweeney, S., Raves, M. L., Harel, M., Gros, P., Silman, I., Kroon, J. & Sussman, J. L. (2000). *Proc. Natl Acad. Sci. USA*, **97**, 623–628.

Weik, M., Ravelli, R. B., Silman, I., Sussman, J. L., Gros, P. & Kroon, J. (2001). *Protein Sci.* **10**, 1953–1961.

electronic reprint